LEO-PNT Performance Metrics: An Extensive Comparison Between Different Constellations

Kaan Çelikbilek[1,*], Elena Simona Lohan[1]

[1]*Tampere University, Korkeakoulunkatu 7, 33720, Tampere, Finland*

Abstract

Recent years have shown that Low-Earth Orbit (LEO) satellites are becoming the leading idea for the future of the space industry, gathering heavy investment from technology giants, as seen from several providers of mega-constellations, such as SpaceX (Starlink), Eutelsat (OneWeb), Iridium, or Amazon (Kuiper). LEO satellites are suitable not only for communication purposes, but they also hold a strong potential for Positioning, Navigation and Timing (PNT) applications, as their proximity to Earth results in fast satellite movements in orbit as well as in high received signal strengths, which may translate into better PNT signals compared to already available alternatives. In this work, we show the viability of LEO-PNT constellations by providing a comprehensive performance comparison based on coverage, Dilution of Precision (DOP) and Carrier-to-Noise Ratio (C/N_0) metrics between several existing and upcoming constellations, as well as two theoretical LEO-PNT constellations, by considering them as dedicated LEO-PNT systems. Our results show that, among the existing and upcoming LEO constellations, Starlink, OneWeb, Xona and Centispace show great promise for future PNT solutions, and that alternative designs that are on par, or perhaps even better, are still possible.

Keywords

LEO Constellations, GNSS Positioning, LEO-PNT, Constellation Comparison, Link Budget Simulation

1. Introduction

1.1. Motivation for LEO-PNT Systems

Technological advances in satellite technologies have opened up the possibility of cheaper and bulk satellite production, i.e., in the form of CubeSats [1, 2, 3, 4], which makes the concept of Low-Earth Orbit (LEO)-based applications a highly promising and exciting new area of business and research. From academia to industry, many players are interested in designing, launching, or innovating the existing and upcoming LEO satellites, with promises to transform our everyday habits. Possible applications of LEO systems are to offer broadband connectivity globally, to enable leading scientific research in fields within the space industry, to offer Earth-sensing solutions, and, more recently, to complement the existing Global Navigation Satellite Systems (GNSS) for robust and seamless navigation. There are already thousands of satellites launched in LEO orbits placed between 200 and 2000 km above the Earth [5, 6] and these satellites support various communication [7, 8, 9, 10], remote sensing [11] and Earth sensing applications [12, 13]. It is expected that the number of LEO satellites will continue to increase at a fast pace in the near future due to the fast time-to-market and lower launching costs compared to Medium Earth Orbit (MEO) and Geosynchronous Equatorial Orbit (GEO) satellite launches. The suitability of LEO satellites as Positioning, Navigation and Timing (PNT) solutions however, has not yet been addressed extensively in the current literature and it has started to gain momentum only in the past few years. Currently, global positioning solutions rely heavily on GNSS, which are susceptible to malicious interferences. Therefore, there is a timely need of complementary, or even alternative, global, and preferably low-cost, positioning methods. The Low-Earth Orbit-based Positioning, Navigation, and Timing (LEO-PNT) concept is the perfect candidate due to LEO satellite's proximity to Earth, which translates to stronger signals compared to MEO and GEO signals at similar carrier frequencies, their

capability for global coverage, and their potential for flexible, scenario-specific designs, e.g. through optimization methods [14]. These new LEO signals could be exploited for PNT in the inevitable event that GNSS signals become either unavailable (e.g., in deep urban canyons, under dense foliage, during long periods of interferences) or untrustworthy (e.g., under malicious spoofing attacks).

1.2. Current LEO Landscape

The current LEO landscape includes new constellations such as Centispace [15, 16] and Xona [17], as well as older constellations such as Orbcomm [18], Iridium [19], Globalstar [20], Starlink [8], or Kuiper [10]. These constellations have potential for PNT services, either as signals of opportunity (e.g., Iridium, Starlink) or as dedicated PNT systems (e.g., Centispace, Xona). Although many aspects of these constellations are not public knowledge, either due to legal concerns or due to design uncertainties, research is being conducted for the different parts of LEO satellite systems in a speedy manner. For LEO-PNT applications, research work have mostly been focused on integrated LEO and GNSS solutions [21, 22], as well as on meta-signals and opportunistic signal frameworks [23, 24] and on alternative positioning based on Doppler integration [25, 26]. In [27], the authors combine these three focuses and argue that the unknown nature of the LEO satellite signals –due to private operators tendency to not share technical information– make the opportunistic approach a necessity and present their signal model and estimation procedure for multiple scenarios involving multiple-constellation PNT using OneWeb, Iridium NEXT, Starlink, and Orbcomm constellations. Their results show the feasibility of LEO and GNSS integration, as well as Doppler-based positioning implementations together with pseudorange based methods. In addition to PNT solutions, research work on LEO satellites expand to other fields as well, such as generic constellation designs for multi-purpose applications [14, 28], LEO-based applications for autonomous vehicles [29, 30], and LEO network design [31, 32]. The variety of research in possible applications of LEO satellites further shows the potential benefits of LEO-PNT solutions in the relatively near future.

1.3. Paper Goal and Contributions

Motivated by the fact that very few performance comparisons among LEO-PNT constellations have been published so far, we present a simulation-based extensive comparison of several LEO-PNT performance metrics for eight LEO satellite constellations (one as the GNSS benchmark, three selected among existing mega-constellations, two selected among on-going LEO-PNT designs and two experimental ones, based on prior work by the Authors). The comparisons are made with a MATLAB-based [33] in-house developed constellation simulator (see section 2.3), under several indoor/outdoor scenarios. Our main contributions are:

- Providing an extensive performance comparison, based on coverage, Dilution of Precision (DOP), and Carrier-to-Noise Ratio (C/N_0) metrics between nine constellations, based on three types of models: models relying on existing mega-constellations (Kuiper, OneWeb, Starlink), models relying on existing smaller-sized LEO-PNT constellations (Centispace and Xona) and Authors' derived models, based on direct parameter optimization [14, 4]. The European GNSS constellation Galileo is included as a benchmark.
- Discussing the meaning of the obtained results under indoor and outdoor scenarios and emphasizing the open challenges in designing a LEO-PNT system.
- Providing system recommendations on constellation design aspects of possible future LEO-PNT constellations.

Table 1

Parameters of Included Satellite Constellations (as of April 2024)

Constellation	# of Satellites	Altitude [km]	Inclination [deg]	EIRP	Bandwidth	Carrier Frequency
*Kuiper[10]	7774	590-650	33-80	76 dBm	400 MHz	18 GHz
*Starlink Gen-1[7]	4408	540-570	53-97.6	69.1 dBm	250 MHz	12 GHz
*Starlink Gen-2[8]	29988	340-615	33-148	69.1 dBm	250 MHz	12 GHz
*OneWeb[9]	7808	1200	40-88	65 dBm	250 MHz	12 GHz
*CentiSpace[34]	190	975-1100	55-88	**65 dBm	**4.092 MHz	**1561.098 MHz
*Xona[35]	492	**1080	53-90	**65 dBm	**4.092 MHz	**1561.098 MHz
Experimental 1 [14]	280	825	72	69.1 dBm	10 MHz	12 GHz
Experimental 2 [4]	420	600	76	69.1 dBm	10 MHz	12 GHz
Galileo[36]	27	23222	56	59 dBm	24.552 MHz	1575.42 MHz

* : These constellations have multiple-shells, and the indicated altitude and inclination ranges mean that individual shells have particular values for that parameter which falls between the given ranges.

** : These parameters are based on our assumptions as exact values could not be found in public resources.

2. Methodology and Target Performance Metrics

2.1. Relevant Constellations

As mentioned in subsection 1.3, our study uses the Galileo constellation as the GNSS benchmark, and includes 7 known LEO constellations: 3 mega constellations, 2 smaller-scale constellations, and 2 experimental ones. Even if possibly outdated, the constellation parameters (i.e., orbital altitude, number of satellites, number of orbital planes, phasing angle between orbital planes, inclination angle of the orbital plane, constellation topology, Right Ascension of the Ascending Node (RAAN) and eccentricity) for the existing constellations can be obtained from public sources, with some exceptions. Most of the relevant parameters for Xona were published in their patent application [35], however a few parameters, i.e. the altitude and satellite's exact operating Effective Isotropic Radiated Power (EIRP), are not given exactly. In a similar manner, to the best of the Authors' knowledge, the exact channel parameters for Centispace are also not available publicly. Therefore, some assumptions were made as seen in Table 1 in order to fill the gaps. Since Centispace has been designed as an augmentation system for Beidou, we assume that the missing parameters are similar to Beidou's B1 band. As for Xona, the orbital plane altitude is taken as the mentioned upper limit from [35], and the channel parameters are again assumed to be similar to Beidou's for comparison purposes with Centispace's constellation design.

In addition to the mentioned known constellations, we provide 2 experimental single-shell LEO-PNT constellation designs, that have been obtained in our earlier studies [4, 14] that we name; i) "Experimental 1", and ii) "Experimental 2". The important parameters for all the relevant constellations that we selected for our comparisons are seen in Table 1. The Starlink constellation includes two generations: Gen-1 refers to the satellites launched according to the initial constellation design from 2018 and Gen-2 refers to the satellites launched during 2020-2022 with an alternate design.

2.2. LEO-PNT Metrics

In order to evaluate the performance of LEO-PNT constellations we selected metrics that are related to the geometry between the users and the satellites, as well as to the reception quality of the received signal. The metrics that we selected for our comparisons are: coverage, Geometric Dilution of Precision (GDOP), Position (3D) Dilution of Precision (PDOP) and C/N_0.

The coverage reflects the signal-reception percentage; for most PNT solutions, a good reception requires having at least 4 satellites in view, i.e., 4-fold coverage. However, not every constellation we use in our comparison is PNT focused, and may not be optimized for 4-fold coverage. Thus, we compute both 4-fold and 1-fold coverage: the coverage here is computed as the percentage of the number of users that have at least 4 and 1 satellites in view, respectively. The GDOP and PDOP are DOP metrics

that reflect the geometry of the user and the constellation [37]; the PDOP reflects the 3D position accuracy and the GDOP reflects the joint 3D position-and-timing accuracy. Similarly, the C/N_0 reflects the quality of the received signal, and it is calculated via eq. (1), where B_w is the bandwidth of the channel, and Signal-to-Noise Ratio (SNR) is calculated for each satellite-user pair.

$$C/N_0^{dB-Hz} = SNR + 10log_{10}(B_w) \tag{1}$$

A high PNT performance with respect to these metrics is reached for high 4-fold coverage, low values for DOP metrics, and high values for C/N_0.

2.3. Simulation Environment

In our previous works [4, 14], a detailed LEO constellation simulator has been developed in MATLAB for LEO-PNT performance analysis, combining MATLAB libraries with the external QuaDRiGa channel library [38], used for the link-budget modelling. Our simulator mimics a satellite constellation from a set of inputs: the constellation parameters, the start time and the duration of the simulation, and the user information (i.e., position and velocity vectors at each time instant and number of users placed according to a uniform distribution on Earth). In addition, a secondary set of input parameters are provided for QuaDRiGa models, which includes: satellite EIRP, receiver sensitivity, atmospheric attenuation effects, and scenario information. We performed simulations for 2 different receiver sensitivity values; i) -125 dBm, representing the low-sensitivity case, and ii) -185 dBm, representing the high-sensitivity case, under 6 different scenarios provided by the QuaDRiGa library that correspond to different Line of Sight (LOS) and Non-Line of Sight (NLOS) conditions:

- "Indoor 1 (I-1)"; Indoor, Rural and NLOS
- "Indoor 2 (I-2)"; Indoor, Urban and NLOS
- "Outdoor 1 (O-1)"; Outdoor, Urban and NLOS
- "Outdoor 2 (O-2)"; Outdoor, Urban and LOS
- "Outdoor 3 (O-3)"; Outdoor, Rural and LOS
- "Outdoor 4 (O-4)"; Outdoor, Rural and NLOS

The simulations consider users uniformly spread on Earth and stationary, and rural/urban choice changes the number of channel clusters and paths, as well as parameters related to large-scale fading decorrelation distances and inter-parameter correlations within QuaDRiGa. Indoor scenarios are considered with 50 meter penetration. Constellations are initialized according to their own parameters as in Table 1. Each simulation has a duration of 1 hour with 1 minute samples, meaning 600 Monte-Carlo runs per satellite in the constellation. Scenarios assume summer conditions for the atmospheric models. 3 attenuation models are taken into consideration in the link budget; i) atmospheric absorption, ii) rain, and iii) fog, all calculated via MATLAB's internal functions. We assume light rain with 2.5 mm/h rate and a cloud liquid water density of 0.5 g/m3. Temperature (T), dry air pressure (p) and water-vapor density (ρ) are modeled from the satellite altitude (h), as given in equations (2), (3) and (4) respectively [39].

$$T(h) = 286.8374 - 4.7805h - 0.1402h^2 \quad [K] \tag{2}$$

$$p(h) = 1008.0278 - 113.2494h + 3.9408h^2 \quad [hPa] \tag{3}$$

$$\rho(h) = 8.988 \exp(-03614h - 0.005402h^2 - 0.001955h^3) \quad [g/m3] \tag{4}$$

3. Comparative Results and Discussion

Tables 2 and 3 show the results of the simulations for high and low sensitivity cases respectively, providing LEO-PNT metrics averaged over the Monte-Carlo runs. The immediate thing to notice between the two tables is the coverage difference; as expected, the coverage is significantly higher in high-sensitivity than in low-sensitivity case for all constellations. Further examining the coverage values, we see that:

i In Table 3, the cases with 0% 4-fold coverage show the GDOP, PDOP, C/N_0 and the received power values as N/A, meaning not applicable, as DOP metrics have no physical meaning outside of instances where PNT solutions exist.

ii In instances where the coverage does not change between Tables 2 and 3, the average C/N_0 and received power values are the same (i.e., Starlink O-2), but for instances that change (i.e., Starlink O-1), the better coverage instances include more conditions with weak signals, thus both the average C/N_0 and received power values decrease.

iii It can be seen from Table 3 that Starlink, Xona and Centispace are the constellations that provide resilience to indoor and low sensitivity conditions, and are still able to provide acceptable DOP metrics given the four-fold coverage is achieved. In the less challenging scenarios (O-2, O-3 and O-4), every LEO constellation is able to achieve acceptable metrics in low sensitivity conditions, with Starlink, OneWeb and Xona being able to achieve full coverage. In comparison, Galileo is able to either operate fully, as seen in O-2 and O-3 scenarios, or not able to operate at all due to the low sensitivity of the receivers.

iv Table 2 shows a different picture, that even in high-sensitivity conditions, it can be challenging to achieve a four-fold coverage. Centispace and the experimental designs show a similar picture; they are able to achieve acceptable LEO-PNT metrics with a relatively low number of LEO satellites, yet they struggle to achieve a complete four-fold coverage; while Xona's design seems to be better performing but still cannot guarantee complete four-fold coverage in all scenarios. Among the mega-constellations, Starlink and OneWeb achieve the best performance and are very similar, with Kuiper falling behind; providing a better LEO-PNT performance compared to the smaller LEO constellations, but failing to achieve a complete four-fold coverage in any scenario. Comparing the rest of Table 2 to the Galileo entry, which serves as the GNSS benchmark, it is clear that similar, if not better, PNT performance can be achieved with the considered LEO constellation designs in comparison.

Galileo values serve as a benchmark and show what metrics are obtained with the current GNSS systems in the considered scenarios, as well as what potential a LEO-PNT constellation has. Values in Table 2 in particular, as the sensitivity allows for very high coverage for almost all designs, show what the main appeal of a dedicated LEO-PNT constellation is over the GNSS constellations; a significant improvement in C/N_0 for the same frequency band, and therefore, the possibility of shifting operations to higher frequency bands, which are less crowded. While the best performing LEO constellation in this study is indeed Starlink, we would like to emphasize that this does not strictly mean that a mega-constellation is necessary to achieve good LEO-PNT services. In fact, the four-fold coverage difference seen between Kuiper, Xona and Centispace shows that simply increasing the number of satellites within a constellation does not directly translate into improved PNT performance. The smaller scale LEO-PNT constellations and the author team's experimental designs provide a more balanced approach between cost/complexity of the constellation and its PNT performance. Their C/N_0 is a direct improvement compared to Galileo, and the DOP metrics, while slightly worse, are still within the same performance range of < 10.

We would like to further demonstrate two aspects via Fig. 1. The first aspect is that, Similar trends are seen for both I-1 and O-2 scenarios. Indoor and outdoor conditions affect the constellations in the same way by lowering their C/N_0 values drastically; which can impact the coverage depending on receiver sensitivity levels. Fig. 1a and 1b show the LEO-PNT metrics of the considered constellations with respect to each other for the high-sensitivity case, for two selected scenarios; I-1 and O-2. Looking at Fig. 1a and 1b, Starlink and Oneweb yields drastically better C/N_0 and GDOP than Galileo while equally maintaining the complete coverage, and Kuiper showing slightly worse C/N_0 and GDOP compared to the other mega-constellations, yet fails to keep up with the complete coverage provided by Galileo. Aside from the mega-constellations, Xona, Centispace and the experimental designs also provide C/N_0 improvements over Galileo. Xona yields a slight improvement with respect to the GDOP, while Centispace and the experimental designs have slightly worse GDOP compared to Galileo, but still remain within good GDOP value ranges. We can also see that the average number of visible satellites are higher compared to Galileo for the mega-constellations, Xona, and the experimental designs, which
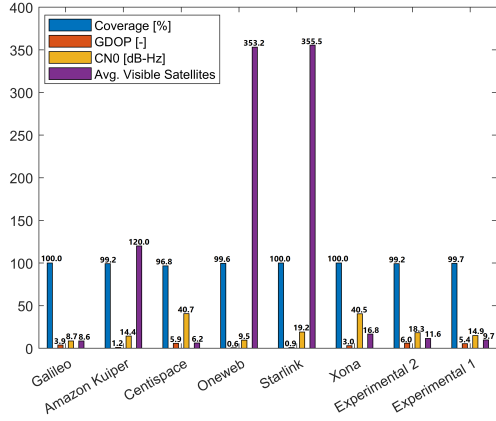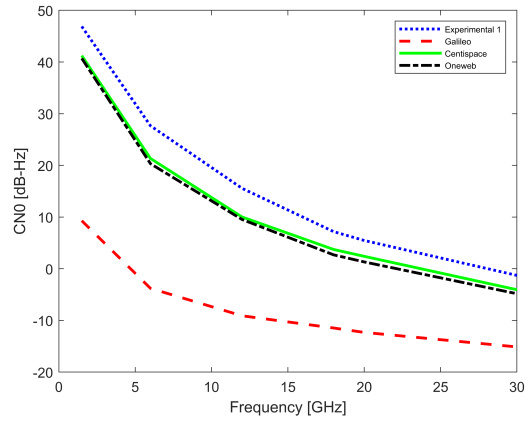
(a) I-1 for -185 dBm
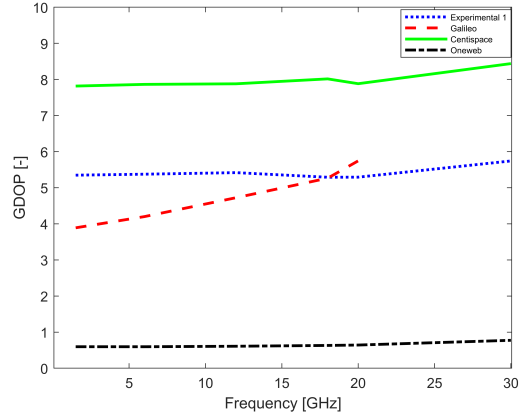
(c) GDOP in I-1 for -185 dBm
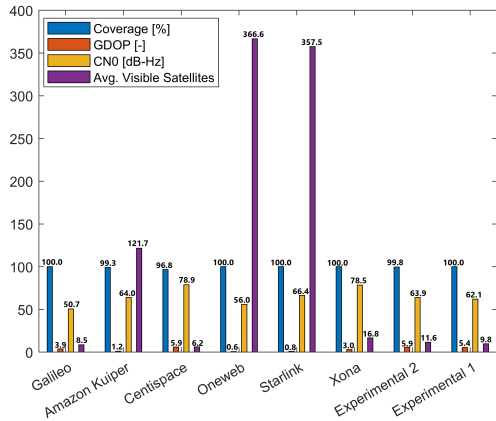
(b) O-2 for -185 dBm

(d) C/N_0 in I-1 for -185 dBm

Figure 1: Left: LEO-PNT metrics for all constellations; Right: GDOP and C/N_0 versus carrier frequency in I-1

imply better stability in cases of satellite failures.

The second aspect is the carrier frequency effect on LEO-PNT. Fig. 1c and 1d presents GDOP and C/N_0 respectively for a subset of four constellations; Galileo, Oneweb, Centispace, and Experimental 1; representing the GNSS benchmark, mega-constellations, small-scale LEO constellations, and potential LEO-PNT constellations respectively. Scenario I-1 is shown as an example, with the observation that similar trends have been noticed for O-2 scenario as well. The GDOP is not influenced much by the carrier frequency, with the exception of Galileo, whose signals fail to penetrate the indoor scenario with enough strength to be received by the receiver after around 20 GHz. On the other hand, C/N_0 drops in a consistent manner as for all constellations as the carrier frequency increases. Together, this shows us that going above X-band or Ku-band for the carrier frequency would risk operational failure for GNSS systems, while LEO-PNT systems would be able to support up to Ka-band carrier frequencies. We note that LEO constellations operating in K-band can reach to the same C/N_0 values that the GNSS constellations have in L-band, and that if the same carrier frequency is used, the improvement is significant in favor of the LEO constellations versus Galileo, and GNSS by extension.

4. Conclusion

This article has shown an extensive comparison between seven LEO satellite constellations and Galileo constellation as the GNSS benchmark (provided in Table 1) in terms of LEO-PNT metrics. We selected the coverage, the GDOP, and the C/N_0 as relevant LEO-PNT performance metrics to be in used comparisons. Using a MATLAB simulation created in-house for analysis, Tables 2 and 3 detail the

impact of different scenarios and receiver sensitivities on these performance metrics. Indoor/outdoor, rural/urban, and LOS/NLOS scenarios are considered in the link budget, and compared for low (i.e., -125 dBm) versus high (i.e., -185 dBm) receiver sensitivity cases. We show that, among the available and upcoming LEO constellations, Starlink, OneWeb, and Xona are the most promising for future LEO-PNT applications. We also show that experimental designs that can reach similar GDOP and coverage performance as Galileo (and GNSS by extension) are possible, which provide a direct improvement on C/N_0. This fact also hints at the possibility that alternative LEO-PNT constellation designs can be further optimized for even better LEO-PNT solutions.

Acknowledgments

References

[1] A. Zeedan, T. Khattab, Cubesat communication subsystems: A review of on-board transceiver architectures, protocols, and performance, IEEE Access 11 (2023) 88161–88183. doi:10.1109/ACCESS.2023.3304419.

[2] M. Centenaro, C. E. Costa, F. Granelli, C. Sacchi, L. Vangelista, A survey on technologies, standards and open challenges in satellite iot, IEEE Comm. Surveys & Tutorials 23 (2021) 1693–1720. doi:10.1109/COMST.2021.3078433.

[3] I. F. Akyildiz, A. Kak, S. Nie, 6G and beyond: The future of wireless communications systems, IEEE Access 8 (2020). doi:10.1109/ACCESS.2020.3010896.

[4] R. Morales Ferre, J. Praks, G. Seco-Granados, E. S. Lohan, A feasibility study for signal-in-space design for LEO-PNT solutions with miniaturized satellites, IEEE Journal on Miniaturization for Air and Space Systems 3 (2022) 171–183. doi:10.1109/JMASS.2022.3206023.

[5] U. of Concerned Scientists, UCS satellite database, 2023. URL: https://www.ucsusa.org/resources/satellite-database.

[6] J. C. McDowell, The low earth orbit satellite population and impacts of the SpaceX Starlink constellation, The Astrophysical Journal Letters 892 (2020) L36. doi:10.3847/2041-8213/ab8016.

[7] Starlink, SpaceX non-geostationary satellite system - technical information to supplement schedule, 2020. URL: https://fcc.report/IBFS/SAT-MOD-20200417-00037/2274316.pdf.

[8] Starlink, Amendment to pending application for the SpaceX gen2 NGSO satellite system, 2021. URL: https://fcc.report/IBFS/SAT-AMD-20210818-00105/12943361.pdf.

[9] Y. Henri, The OneWeb Satellite System, Handbook of Small Satellites: Technology, Design, Manufacture, Applications, Economics and Regulation, Springer, Cham, 2020, pp. 1–10. doi:10.1007/978-3-030-20707-6_67-1.

[10] K. S. LLC, Application of Kuiper systems LLC for authority to launch and operate a non-geostationary satellite orbit system in ka-band frequencies: Technical appendix, 2021. URL: https://apps.fcc.gov/els/GetAtt.html?id=285359&x=.

[11] FCC, Exhibit 1 - FCC form 442 / HawkEye 360 Pathfinder Cluster / item 7 and 8: Purpose of experiment and duration, 2020. URL: https://apps.fcc.gov/els/GetAtt.html?id=186545&x=.

[12] ESA, ICEYE ESA archive, about ICEYE, 2023. URL: https://earth.esa.int/eogateway/missions/iceye.

[13] H. J. Krame, Blacksky constellation, 2016. URL: https://www.eoportal.org/satellite-missions/blacksky-constellation.

[14] K. Çelikbilek, Z. Saleem, R. Morales Ferre, J. Praks, E. S. Lohan, Survey on optimization methods

for LEO-satellite-based networks with applications in future autonomous transportation, Sensors 22 (2022). doi:10.3390/s22041421.

[15] L. Yang, The Centispace-1: A LEO satellite-based augmentation system, in: 14th Meeting of the International Committee on Global Navigation Satellite Systems, International Committee on GNSS (ICG), 2019, pp. 342–352. Accessed on: June 25, 2024.

[16] Z. Yang, H. Liu, C. Qian, B. Shu, L. Zhang, X. Xu, Y. Zhang, Y. Lou, Real-time estimation of low earth orbit (LEO) satellite clock based on ground tracking stations, Remote Sensing 12 (2020). doi:10.3390/rs12122050.

[17] X. S. Systems, Xona Space PULSAR constellation description, 2022. URL: https://www.xonaspace.com/pulsar.

[18] J. Harms, The Orbcomm experience, 2004. URL: https://artes.esa.int/sites/default/files/1_The_Orbcomm_Experience.pdf.

[19] C. Fossa, R. Raines, G. Gunsch, M. Temple, An overview of the IRIDIUM (R) low earth orbit (LEO) satellite system, in: Proceedings of the IEEE 1998 National Aerospace and Electronics Conference. NAECON 1998. Celebrating 50 Years (Cat. No.98CH36185), IEEE, IEEE, 1998, pp. 152–159. doi:10.1109/NAECON.1998.710110.

[20] F. J. Dietrich, P. Metzen, P. Monte, The Globalstar cellular satellite system, IEEE Transactions on Antennas and Propagation 46 (1998) 935–942. doi:10.1109/8.686783.

[21] T. Reid, T. Walter, P. Enge, D. Lawrence, H. Cobb, G. Gutt, M. O'Connor, D. Whelan, Navigation from low earth orbit–part 1: Concept, current capability, and future promise, in: J. Morton, F. van Diggelen, J. J. Spilker, B. Parkinson (Eds.), Position, Navigation, and Timing Technologies in the 21st Century, volume 2, John Wiley & Sons, Ltd, 2021, pp. 1359–1379. doi:10.1002/9781119458555.ch43a.

[22] M. Hartnett, Performance Assessment of Navigation Using Carrier Doppler Measurements from Multiple LEO Constellations, Master's thesis, Air Force Institute of Technology, Ohio, USA, 2022.

[23] Z. Kassas, Navigation from low earth orbit–part 2: Models, implementation, and performance, in: J. Morton, F. van Diggelen, J. J. Spilker, B. Parkinson (Eds.), Position, Navigation, and Timing Technologies in the 21st Century, volume 2, John Wiley & Sons, Ltd, 2021, pp. 1381–1412. doi:10.1002/9781119458555.ch43b.

[24] A. Nardin, F. Dovis, J. A. Fraire, Empowering the tracking performance of LEO-based positioning by means of meta-signals, IEEE Journal of RF Identification 5 (2021) 244–253. doi:10.1109/JRFID.2021.3077082.

[25] M. Neinavaie, J. J. Khalife, Z. Kassas, Blind doppler tracking and beacon detection for opportunistic navigation with LEO satellite signals, 2021 IEEE Aerospace Conference (50100) (2021) 1–8. doi:10.1109/AERO50100.2021.9438258.

[26] C. Zhao, H. Qin, Z. Li, Doppler measurements from multiconstellations in opportunistic navigation, IEEE Transactions on Instrumentation and Measurement 71 (2022) 1–9. doi:10.1109/TIM.2022.3147315.

[27] Z. Kassas, S. Kozhaya, J. Saroufim, H. Kanj, S. Hayek, A look at the stars: Navigation with multi-constellation LEO satellite signals of opportunity, Inside GNSS (2023).

[28] J. Saroufim, S. W. Hayek, Z. M. Kassas, Simultaneous LEO satellite tracking and differential LEO-aided IMU navigation, in: 2023 IEEE/ION Position, Location and Navigation Symposium, 2023, pp. 179–188. doi:10.1109/PLANS53410.2023.10140087.

[29] Y. Li, H. Li, W. Liu, L. Liu, W. Zhao, Y. Chen, J. Wu, Q. Wu, J. Liu, Z. Lai, H. Qiu, A Networking Perspective on Starlink's Self-Driving LEO Mega-Constellation, 17, Association for Computing Machinery, New York, NY, USA, 2023, pp. 1–16. doi:10.1145/3570361.3592519.

[30] T. G. Reid, B. Chan, A. Goel, K. Gunning, B. Manning, J. Martin, A. Neish, A. Perkins, P. Tarantino, Satellite navigation for the age of autonomy, in: 2020 IEEE/ION Position, Location and Navigation Symposium (PLANS), IEEE, IEEE, 2020, pp. 342–352.

[31] K. Zhang, L. Tang, C. Zhao, S. Zhong, H. Luo, Perfect hash-based routing lookup for LEO constellation backbone network, IEEE Transactions on Aerospace and Electronic Systems 59 (2023) 4844–4857. doi:10.1109/TAES.2023.3244897.

[32] S. Ma, Y. C. Chou, H. Zhao, L. Chen, X. Ma, J. Liu, Network characteristics of LEO satellite constellations: A Starlink-based measurement from end users, in: IEEE INFOCOM 2023 - IEEE Conference on Computer Communications, 2023, pp. 1–10. doi:10.1109/INFOCOM53939.2023.10228912.

[33] T. M. Inc., MATLAB version: 9.13.0 (r2022b), 2022. URL: https://www.mathworks.com.

[34] M. Xu, Centispace system experimental satellites PPP application test, in: Proceedings of the 2023 UN/Finland Workshop on GNSS, 2023, pp. 1–21. Accessed on: June 25, 2024.

[35] X. S. S. Inc., Satellite for transmitting a navigation signal in a satellite constellation system, 2021. URL: https://patents.justia.com/patent/11668834.

[36] E. S. A. (ESA), Galileo satellites, 2022. URL: https://www.esa.int/Applications/Navigation/Galileo/Galileo_satellites.

[37] E. S. Lohan, K. Borre, Accuracy limits in multi-GNSS, IEEE Transactions on Aerospace and Electronic Systems 52 (2016) 2477–2494. doi:10.1109/TAES.2016.150241.

[38] S. Jaeckel, L. Raschkowski, K. Börner, L. Thiele, QuaDRiGa: A 3-D multi-cell channel model with time evolution for enabling virtual field trials, IEEE Transactions on Antennas and Propagation 62 (2014) 3242–3256. doi:10.1109/TAP.2014.2310220.

[39] W. Wang, E. S. Lohan, J. Talvitie, MmWave solutions to cope with the data link challenges in aviation, Deliverable D4.3 within H2020-SESAR-2016-2, EMPHASIS, 2019.

Table 2
LEO-PNT Performance Metrics for -185 dBm Receiver Sensitivity (high sensitivity)

Constellation	Scenario	Coverage [%]		GDOP [-]	PDOP [-]	C/N_0 [dB-Hz]	Received Power [dB]	Path-Loss [dB]
		4-Fold	1-Fold					
Galileo	I-1	100	100	3.88	3.34	8.67	-160.30	226.88
	I-2	94.77	96.94	4.04	3.48	0.64	-168.34	236.43
	O-1	100	100	3.86	3.31	24.80	-144.18	210.68
	O-2	100	100	3.85	3.31	50.66	-118.32	184.82
	O-3	100	100	3.85	3.31	51.07	-117.91	184.41
	O-4	100	100	3.85	3.31	33.93	-135.04	201.54
Kuiper	I-1	99.23	99.25	1.18	1.05	14.39	-154.59	238.53
	I-2	96.48	96.88	1.32	1.17	3.27	-165.70	252.01
	O-1	99.27	99.29	1.18	1.05	35.27	-133.71	217.21
	O-2	99.27	99.29	1.17	1.04	64.05	-104.93	188.43
	O-3	99.27	99.29	1.18	1.05	64.34	-104.63	188.13
	O-4	99.27	99.29	1.18	1.04	48.37	-120.61	204.11
OneWeb	I-1	99.58	99.63	0.61	0.54	9.55	-159.43	233.00
	I-2	93.15	93.92	0.63	0.56	0.45	-168.53	244.89
	O-1	100	100	0.60	0.53	28.85	-140.12	212.62
	O-2	100	100	0.60	0.53	56.00	-112.97	185.47
	O-3	100	100	0.60	0.53	56.32	-112.66	185.16
	O-4	100	100	0.60	0.53	40.96	-128.01	200.51
Starlink	I-1	100	100	0.89	0.80	19.16	-149.81	226.59
	I-2	99.38	99.46	0.90	0.81	7.58	-161.40	239.21
	O-1	100	100	0.86	0.77	39.40	-129.58	206.18
	O-2	100	100	0.84	0.75	66.43	-102.55	179.15
	O-3	100	100	0.83	0.73	66.73	-102.25	178.85
	O-4	100	100	0.84	0.74	51.53	-117.45	194.05
Centispace	I-1	96.77	100	5.94	5.31	40.70	-128.27	200.77
	I-2	96.77	100	5.93	5.29	32.28	-136.70	209.20
	O-1	96.77	100	5.93	5.31	57.57	-111.41	183.91
	O-2	96.77	100	5.95	5.31	78.89	-90.09	162.59
	O-3	96.77	100	5.94	5.31	79.24	-89.73	162.23
	O-4	96.77	100	5.93	5.31	65.39	-103.59	176.09
Xona	I-1	100	100	3.03	2.71	40.49	-128.49	200.99
	I-2	100	100	3.05	2.71	32.32	-136.65	209.16
	O-1	100	100	3.03	2.71	57.31	-111.67	184.17
	O-2	100	100	3.05	2.73	78.53	-90.44	162.94
	O-3	96.9	100	3.04	2.72	78.89	-90.09	162.59
	O-4	100	100	3.04	2.72	65.11	-103.86	176.36
Experimental 1	I-1	99.71	100	5.36	4.77	14.94	-154.03	230.73
	I-2	93.10	95.48	5.27	4.67	3.78	-165.19	242.98
	O-1	99.98	100	5.37	4.76	34.84	-134.13	210.73
	O-2	100	100	5.37	4.78	62.09	-106.89	183.49
	O-3	100	100	5.37	4.78	62.40	-106.57	183.17
	O-4	99.98	100	5.36	4.76	47.07	-121.90	198.50
Experimental 2	I-1	99.19	100	5.98	5.36	18.34	-150.64	227.32
	I-2	92.5	97.15	5.89	5.27	7.20	-161.77	240.10
	O-1	99.71	100	5.91	5.32	37.06	-131.91	208.51
	O-2	99.75	100	5.92	5.33	63.95	-105.03	181.63
	O-3	99.75	100	5.93	5.33	64.25	-104.72	181.32
	O-4	99.75	100	5.94	5.32	49.19	-119.78	196.38

Table 3

LEO-PNT Performance Metrics for −125 dBm Receiver Sensitivity (low sensitivity)

Constellation	Scenario	Coverage [%]		GDOP [-]	PDOP [-]	C/N_0 [dB-Hz]	Received Power [dB]	Path-Loss [dB]
		4-Fold	1-Fold					
Galileo	I-1	0	0.38	N/A	N/A	N/A	N/A	226.88
	I-2	0	0.38	N/A	N/A	N/A	N/A	236.43
	O-1	0	0.38	N/A	N/A	N/A	N/A	210.68
	O-2	100	100	3.86	3.31	50.66	−118.32	184.82
	O-3	100	100	3.85	3.30	51.07	−117.91	184.41
	O-4	0	0.60	N/A	N/A	N/A	N/A	201.54
Kuiper	I-1	0	3.21	N/A	N/A	N/A	N/A	238.53
	I-2	0	1.19	N/A	N/A	N/A	N/A	252.01
	O-1	0	5.02	N/A	N/A	N/A	N/A	217.21
	O-2	99.27	99.29	1.18	1.05	64.05	−104.93	188.43
	O-3	99.27	99.29	1.18	1.05	64.34	−104.63	188.13
	O-4	99.27	99.29	1.28	1.14	48.38	−120.60	204.11
OneWeb	I-1	0	2.15	N/A	N/A	N/A	N/A	233.00
	I-2	0	1.67	N/A	N/A	N/A	N/A	244.89
	O-1	0	2.23	N/A	N/A	N/A	N/A	212.62
	O-2	100	100	0.60	0.53	56.00	−112.97	185.47
	O-3	100	100	0.60	0.53	56.32	−112.66	185.16
	O-4	100	100	3.46	2.72	45.39	−123.58	200.51
Starlink	I-1	5.81	9.96	4.17	3.34	46.80	−122.18	226.59
	I-2	0	1.94	N/A	N/A	N/A	N/A	239.11
	O-1	80	81.52	3.47	2.79	45.75	−123.22	206.18
	O-2	100	100	0.87	0.78	66.43	−102.55	179.15
	O-3	100	100	0.86	0.77	66.73	−102.25	178.85
	O-4	100	100	0.91	0.82	51.55	−117.43	194.05
Centispace	I-1	33.04	70.35	7.67	6.83	51.08	−117.90	200.77
	I-2	8.06	34.27	5.68	4.86	48.06	−120.92	209.20
	O-1	96.52	100	5.97	5.28	57.59	−111.39	183.91
	O-2	96.77	100	5.93	5.31	78.89	−90.09	162.59
	O-3	96.77	100	5.93	5.31	79.24	−89.73	162.23
	O-4	96.77	100	5.88	5.27	65.39	−103.59	176.09
Xona	I-1	55.65	72.92	5.91	5.12	49.99	−118.98	200.99
	I-2	19	40.77	8.33	7.26	48.16	−120.81	209.16
	O-1	100	100	3.14	2.78	57.34	−111.64	184.17
	O-2	100	100	3.03	2.71	78.53	−90.44	162.94
	O-3	100	100	3.03	2.71	78.89	−90.09	162.59
	O-4	100	100	3.05	2.72	65.11	−103.86	176.36
Experimental 1	I-1	0	0	N/A	N/A	N/A	N/A	230.73
	I-2	0	0	N/A	N/A	N/A	N/A	242.98
	O-1	0	0	N/A	N/A	N/A	N/A	210.73
	O-2	99.98	100	5.37	4.78	62.09	−106.89	183.49
	O-3	99.98	100	5.37	4.78	63.12	−106.57	183.17
	O-4	87.67	100	5.27	4.72	47.05	−121.92	198.50
Experimental 2	I-1	0	2.56	N/A	N/A	N/A	N/A	227.32
	I-2	0	0.04	N/A	N/A	N/A	N/A	241.10
	O-1	0	8.23	N/A	N/A	N/A	N/A	208.51
	O-2	99.67	100	5.94	5.35	63.95	−105.03	181.63
	O-3	99.67	100	5.93	5.35	64.25	−104.72	181.32
	O-4	91.52	100	6.08	5.40	49.19	−119.78	196.38